THERMAL CONDUCTIVITY OF POLYIMIDE/CARBON NANOFILLER BLENDS

S. Ghose[1], K.A. Watson[2], D.M. Delozier[2], D.C. Working[3], J.W. Connell[3], J.G. Smith[3], Y.P. Sun[4] and Y. Lin[4]

[1]National Research Council Associate at NASA LaRC, Hampton, VA 23681
[2] National Institute of Aerospace, Hampton, VA 23666-6147
[3]NASA Langley Research Center, Hampton, VA 23681-2199
[4]Dept of Chemistry, Clemson University, Clemson, SC 26934-0973

Abstract

In efforts to improve the thermal conductivity of Ultem™ 1000, it was compounded with three carbon based nano-fillers. Multiwalled carbon nanotubes (MWCNT), vapor grown carbon nanofibers (CNF) and expanded graphite (EG) were investigated. Ribbons were extruded to form samples in which the nano-fillers were aligned. Samples were also fabricated by compression molding in which the nano-fillers were randomly oriented. The thermal properties were evaluated by DSC and TGA, and the mechanical properties of the aligned samples were determined by tensile testing. The degree of dispersion and alignment of the nanoparticles were investigated with high-resolution scanning electron microscopy. The thermal conductivity of the samples was measured in both the direction of alignment as well as perpendicular to that direction using the Nanoflash technique. The results of this study will be presented.

Keywords: multiwalled carbon nanotubes, carbon nanofibers, expanded graphite, Ultem 1000™

* To whom correspondence should be addressed: john.w.connell@nasa.gov, (757) 864-4264

1. INTRODUCTION

Combining polymers with an organic or inorganic phase to produce a polymer composite is common in the production and processing of modern plastics. Recently, the use of nanoscale fillers to prepare polymer nanocomposites (PNC) have been investigated to augment the properties of polymers. PNCs are commonly defined as the combination of a polymer matrix resin and inclusions that have at least one dimension in the nanometer size range [1]. PNCs exhibit significant enhancements in certain properties at a far lower concentration than their conventional micro or macro counterparts. Layered clay, expanded graphite, carbon nanofibers and carbon nanotubes are some of the common nanoparticles used in making PNCs.

Carbon nanofibers (CNF) are widely used as reinforcements for polymers in numerous high-technology applications because of their excellent electrical and thermal properties and high specific tensile strength and modulus [2]. Other benefits provided by CNFs include improved heat distortion temperatures and increased electromagnetic shielding. CNFs have been used as reinforcements for various thermoplastics like polyethylene [3], polypropylene [4,5], polycarbonate [6], nylon [7] and poly (methyl methacrylate) [8]. These highly graphitic fibers are produced by a catalytic vapor deposition process and have a wide range of morphologies, from disordered bamboo-like formations [9] to highly graphitized "stacked-cup" structures where conical shells are nested within one another [10]. Additionally, CNFs are generally more economically attractive than carbon nanotubes because of lower manufacturing costs.

Graphite is another material that is commonly used as a filler in polymers. Graphite is one of the stiffest materials found in nature with a Young's modulus of ~1060 MPa and also has excellent thermal and electrical properties. However, utilizing graphite, which exists in large stacks of graphene sheets, necessitates a prior expansion and exfoliation of the graphene layers to obtain particles with nanometer dimensions. With surface treatment of expanded graphite (EG), its dispersion in a polymer matrix results in composites with excellent mechanical and electrical properties and high thermal conductivity. In addition, the material is presently two orders of magnitude less expensive than carbon nanotubes [11]. Electrically conductive nanocomposites were prepared by solution intercalation and master batch melt mixing of high density polyethylene (HDPE)/maleic anhydride grafted polyethylene/ expanded graphite [12]. HDPE was also reinforced with EG and untreated graphite by a melt compounding process that improved electrical and mechanical properties of the EG system [13]. EG has also been made by oxidation of natural graphite followed by thermal expansion and then poly(styrene-co-acrylonitrile)/EG composite sheets have been prepared [14]. Polymethylmethacrylate/EG composites prepared by solution blending methods [15] and aromatic polydisulphide/EG nanocomposites prepared by solution method and hot molding [16] showed good mechanical and electrical properties. The dynamic mechanical and thermal properties of phenylethynyl-terminated polyimide composites reinforced with EG nanoplatelets have also been studied [17].

Carbon nanotube (CNT)-based composites are being studied intensively due to the unique physical/mechanical properties of CNTs. CNTs are thought of as the ultimate carbon fibers, and are expected to have high mechanical and electrical properties and ultra high thermal conductivity [18, 19]. When CNTs are dispersed in polymeric materials, an interconnecting

network is formed which provides a conductive pathway for electrical and/or thermal current to flow. In electrical conductivity the mechanism involves a flow of electrons whereas for thermal conductivity the process of conduction occurs via transfer of phonons. Various methods have been attempted for achieving good dispersion of CNTs in the polymer. They include the preparation of the polymer in the presence of CNTs under sonication [20], the use of alkoxysilane terminated amide acid oligomers to disperse the CNTs [21], melt mixing [22] and shear mixing [23]. Theory predicts the thermal conductivity (κ) of carbon nanotubes at room temperature is as high as ~6600 W/mK [24]. The experimental value of 3000 W/mK for the thermal conductivity of an individual multiwalled carbon nanotube (MWCNT) at room temperature has been reported [25]. This value is significantly higher than that of known thermally conducting materials like diamond (up to 2300 W/mK) and graphite (up to 1960 W/mK). The prominent thermal properties of CNTs have made them promising materials for future applications as thermal management materials. Hence it is reasonable to study the thermal conductivity applications of CNTs. Enhancement of thermal conductivity has been observed in CNT suspensions [26-27]. It is interesting to note that in the case of CNT suspensions, the measured thermal conductivities are generally greater than the theoretical predictions made with conventional heat conduction models. It has been shown in the case of single wall carbon nanotubes (SWCNTs) that thermal conductivities show a peaking behavior before falling off at higher temperatures due to Umklapp scattering [28]. In case of ordinary carbon-carbon composites, there is larger mean free path and less phonon-phonon Umklapp scattering causing the thermal conductivity to increase linearly with heat treatment temperature [29]. However, in PNCs, the improvement in thermal conductivity has always been lower than the rule-of-mixture values.

ULTEM™ was chosen for use as the host resin for trials with the various nanoparticles because the resin is an amorphous thermoplastic polyetherimide offering good melt processability, outstanding high heat resistance, high strength, modulus and broad chemical resistance. For example, SWCNTs have been incorporated (up to 1% by weight) into ULTEM™ and melt processed to yield fibers [30]. Although the melt process was not optimized to fully disperse and align the SWCNTs some improvements in mechanical properties were achieved.

Melt compounding was chosen as the method to disperse the nanoparticles in ULTEM® because it involves high shear mixing which helps to disentangle the nanoparticles and disperse them uniformly within the matrix. Melt mixing was followed by extrusion in the preparation of some of the samples described herein as the process of extruding the nanocomposite through a suitable die and subsequent drawing led to continuous ribbons of nanocomposites with substantial orientation of the nanoparticles in the flow direction. The samples were characterized using differential scanning calorimetry, thermogravimetric analysis, high resolution scanning electron microscopy, mechanical tester and thermal conductivity analyzer. The preparation and characterization of samples containing various loadings of CNTs, CNFs and EGs are discussed.

2. EXPERIMENTAL

2.1 Materials Ultem™ 1000, a melt processable polyimide obtained from GE Plastics, was chosen as the polymer matrix and was used as received. MWCNTs, VGE-S16, were procured

from the University of Kentucky. CNF, Pyrograph – III - PR-24 HHT was obtained from Applied Sciences, Inc and EG (Grade 3775) was received from Asbury Carbons. The graphite already had the galleries expanded by first treating with sulfuric acid and then rapidly heating the sample to 900 ºC. The expansion of the graphite was expected to facilitate exfoliation during melt mixing.

2.2 Processing of Ultem™ 1000 with nanofillers Ultem™ 1000 was compounded with MWCNTs, CNFs and EGs in a 30 cc internal mixer (Plasticorder PL2000, Banbury) for 3 h at 25 rpm, 325 °C under N_2 purge. MWCNTs - 5, 10 and 20 wt%, CNFs - 20, 30 and 40 wt%, and EGs - 20, 30, 40 and 50 wt% were added to the polymer. During mixing the torque produced was used to calculate the viscosity of the sample. Upon completion of mixing the material was ground in a Mini-Granulator (Kayeness, Inc) using a 5.5 mm screen. Samples were extruded through a Laboratory Mixing Extruder (#LME, Dynisco, Inc) at a barrel temperature of 215 °C and a die temperature of 365 °C for the CNF sample, a barrel temperature of 215 °C and a die temperature of 360 °C for the MWCNT sample and a barrel temperature of 190 °C and a die temperature of 350 °C for the EG sample. The dimensions of the die were 0.38 mm x 19.1 mm. The samples were extruded in the form of a continuous ribbon that were 0.1-0.5 mm thick, 10-15 mm wide and several meters in length. Once extruded, the ribbons were cut into pieces approximately 2 cm x 2 cm. They were then stacked on one side of a mold 9 cm x 2 cm x 3 cm (i.d.) and the remainder of the mold filled with Ultem™ pellets. The stacked ribbons were compression molded at 270 °C, 1.72 MPa for 3 h. The molded samples were then sliced using an Isomet low speed saw with a diamond wafering blade 10.2 cm diameter and 0.3 mm thick with 15 HC diamond (Buehler Ltd). Unoriented samples were made using a Laboratory Mixing Molder (#LMM Dynisco, Inc) and a rectangular mold (1.52 mm x 38.1 mm x 1.27 mm). A rough blend of materials was added to the mixing bowl of LMM kept at 360 ^oC and kept there for 0.5 h. It was then dynamically pressed at a rotational speed of 100% of ram-motor capacity and then static pressed to degas, before passing through the nozzle orifice (~1.6mm) into the rectangular mold kept at 360 ^oC. The material was then manually compressed at a pressure of ~ 4.5 kN and set under pressure from the ram while being air cooled.

2.3 Solution mixing of Ultem™ 1000 with nanofillers Solution mixing of the Ultem™ 1000 with MWCNTs was conducted in N,N-dimethylacetamide (DMAc) using a polyimide dispersant, sonication and mechanical (low shear) mixing. The chemical structure of the dispersant is depicted in Figure 1. This polymer aids in the dispersant of the MWCNTs into the host polymer. The experimental procedure is as follows; Into a 500 mL round bottom flask was placed VGE-S12 MWNT (0.75 g) and DMAc (285 mL). This suspension was sonicated for 0.5 h in the Bransonic sonicator. A polyimide dispersant (0.75 g) was added to the suspension and sonicated for 0.5 h with the MWNTs. Ultem™ 1000 was then added in three additions of 5 g each with 0.5 h of sonication between each addition. The mixture was then subjected to overhead stirring for 16 h followed by precipitation into water. The powder was washed one time with 2 L of water and then dried at 100 ºC for 16 h at ambient pressure. The powder was then heated to 150 ºC for 4 h. For CNF samples, approximately 17 g of neat Ultem™ was dissolved in 150 mL hot DMAc. In a separate flask, the required amount of CNF was sonicated in 150 mL DMAc for 1 h and the suspension was subsequently added to the Ultem™ solution. The mixture was stirred at room temperature for 3 h. The mixture was then poured into a blender containing water and the

product collected via vacuum filtration. The product was washed several times in hot water and dried in an air oven at 125 °C for a minimum of 48 h.

2.4 Characterization Differential scanning calorimetry (DSC) was performed on the ribbon samples obtained from extrusion in a sealed aluminum pan using a Shimadzu DSC-50 thermal analyzer at a heating rate of 20 ^{o}C/min with the glass transition temperature (T_g) taken as the mid-point of inflection of the differential heat flow (ΔH) versus temperature curve. Thermogravimetric (TGA) analysis was performed in air (flow rate – 50 mL/min) on the powder samples using an Auto TGA 2950HR (TA Instruments, DE). The samples were heated at 20 ^{o}C/min to 100 ^{o}C, held for 0.5 h to drive off any moisture, and heated to 600 ^{o}C at a rate of 2.5 ^{o}C/min. High-resolution SEM images were obtained using a Hitachi S-5200 field emission scanning electron microscope (FE-SEM) equipped with a "through-the-lens" secondary electron detector. Thin-film tensile properties were determined according to ASTM D882 using either four or five specimens (0.51 cm wide) per test conditions using an Eaton Model 3397-139 11.4 kg load cell on a Sintech 2 test frame. The test specimen gauge length was 5.1 cm and the crosshead speed for film testing was 0.51 cm/minute. Thermal conductivity of the molded samples as well as ribbons was measured using a Netzsch LFA 447 NanoFlash according to ASTM E1461. Samples sizes of 1 cm x 1 cm were sprayed with a thin layer of graphite (for uniform thermal adsorption), which may be easily rinsed away by solvent (e.g., methanol). Pyrex (TC ~ 1.09 W/mK, Cp ~ 0.76 J/gk) was used as the reference.

3. RESULTS AND DISCUSSION

3.1 Processing of Ultem™/nanofillers The torque values were obtained during mixing in the Plasticorder and were used to calculate the melt viscosities of the samples. Table 1 denotes the calculated melt viscosities of the various samples at a shear rate of 92.5 sec^{-1} and a temperature of 325 ° C. It was found that some samples (40 wt% CNF, 50 wt% EG) could not be extruded into ribbons. The difficulty in extruding these samples was due to either their high melt viscosity or the increased thermal conductivity that led to additional heating in the feeding region of the extruder. Figure 2 shows a picture of a typical extruded ribbon. The primary purpose of extrusion was to try and align the nanofillers in the direction of flow. Stacked ribbons were molded and samples were obtained by cutting the molded block in the direction of the dotted line in Figure 3 using a diamond saw. In this way samples were obtained with alignment both parallel and perpendicular to the direction of conductivity measurement.

3.2 HRSEM of extruded ribbons Figure 4(a) shows the image of the 5 wt% MWCNT melt mixed ribbon while Figure 4(b) shows the solution mixed ribbon with the same concentration of MWCNTs. In both cases, it is observed that the MWCNTs are aligned in the direction of flow (indicated by the arrow). Figures 5(a), (b) and (c) show the alignment in at higher MWCNT loading and in CNFs. Figure 5(d) shows the face view of ULTEM™ + 5 wt% MWNT sample. The bumps on the surface indicate the nanotubes in the matrix that are aligned perpendicular to the surface of the sample. HRSEM images were obtained for the 40 wt% EG extruded ribbon (Figure 6). The graphite platelets were visible at high voltages. The platelets vary in size but are all under 1 micron in one dimension. The platelets appear to be very thin which indicates that

exfoliation is taking place during the melt mixing. The particles appeared well dispersed throughout the polymer.

3.3. Mechanical properties of extruded ribbons Mechanical properties were measured on Ultem™/nanofiller composites with the results shown in Table 2. The strips used for testing were cut from ribbons that were prepared from extrusion; hence the nanofillers are somewhat in alignment in the direction of the stress. The 5 wt% MWCNT solution-mixed sample and the 40 wt% EG melt mixed sample did not provide ribbons of sufficient quality for mechanical testing. The other results should be viewed with care because the measurement of the ribbon thickness is not accurate due to uneven ribbon surfaces. The sample with 10 wt% MWCNT solution-mixed method is an example, where the measured thickness of the ribbon is greater than the "average" thickness of the ribbon, resulting in depressed mechanical properties. Typically it has been observed that the melt mixed samples exhibited superior mechanical properties, both modulus and strength, compared to the solution mixed samples. As expected, with increased filler loading level, the modulus increased and the elongation decreased.

3.4 Thermal characterization of extruded ribbons Table 3 denotes the glass transition temperatures (T_g) of the various samples. In case of the MWCNT filled samples, the solution mixed composites exhibited a sharp decrease in T_gs for the 10 and 20 wt% loadings. The melt-mixed composites had negligible changes in T_gs. But in the cases of CNFs and EGs, samples showed very little change in T_gs. The addition of nanofillers improved the temperature of 5 wt% loss as determined by TGA. Neat Ultem™ lost 5 wt% at ~ 480 °C while the filled samples lost the same weight at temperatures > 500 °C. No significant differences in thermo-oxidative stability were observed for the melt-mixed and solution-mixed samples.

3.5 Thermal conductivity measurements Since the structure of nanotubes is anisotropic in space, the electrical and thermal properties should be different in the longitudinal (parallel to nanotube axis) and transverse (perpendicular to nanotube axis) directions. There have been a few reports on the use of dispersed CNTs as thermally conducting fillers in polymer composites and certain enhancements in thermal conductivity were observed [24, 31]. However, the enhanced values are typically below those predicted by the rule of mixtures. One probable reason for this is the existence of interface thermal resistance between the overlaps in the CNT passage leading to a rapid increase in overall thermal resistance [32]. Huang et al. [31] proposed a composite structure where all the CNTs embedded in the matrix are aligned from one surface to the opposite side with all the CNT surfaces revealed on both surfaces. This leads to high thermal conductivity since the CNTs form ideal thermally conducting pathways. Low thermal interface resistances can also be expected as the protruding tips would ensure better thermal contact. It has been reported that alignment of nanofillers in the polymer matrix leads to enhancement of thermal conductivity [29, 33]. Based on the literature survey done so far, it was decided to process samples with significant nanofiller alignment and measure thermal conductivity both in the direction and perpendicular to the direction of alignment (nanotube axis).

Three types of Ultem™/nanofiller samples were measured for thermal conductivity. These were the extruded ribbon, molded samples cut perpendicular to flow direction, and samples with no alignment. For the extruded ribbons the thermal conductivity was measured perpendicular to the

direction of nanotube alignment. Table 4a denotes the values for neat Ultem™ and Ultem™/nanofiller samples. With the exception of the 10 wt% MWCNT sample, the solution mixed ribbons had a slightly higher thermal conductivity than the melt mixed ones. The thermal conductivity increased with increase in loading level of nanofillers. The highest thermal conductivity was observed in the 30 wt% CNF samples and the conductivity was increased by 180% with respect to the neat material. The second set of samples was the molded samples where the thermal conductivity was measured in the direction of nanofiller alignment. Table 4b shows the values for the neat molded sample as well as Ultem™/nanofiller samples. This data has also been shown in a plot (Figure 7). In this case the melt-mixed samples showed a higher thermal conductivity compared to solution mixed ones. The thermal conductivity of the samples were observed to be significantly greater in the direction of alignment (Table 4b) compared to those that were perpendicular to the direction of alignment (Table 4a). The MWCNT samples at 20 wt% loading exhibited an 11.5-fold increase in thermal conductivity relative to neat Ultem™ whereas the CNF samples loaded at 30 wt% showed a 15-fold increase. The largest increase was exhibited by 40 wt% loading of EG samples which showed a 38-fold increase. The data indicates that the nanofillers, when aligned, form a network that successfully conducts heat by enabling a more efficient phonon transfer from one filler particle to another. Finally when it comes to the unoriented samples (Table 4c), it was found that 40 wt% CNF filled samples showed a 10-fold increase while the 50 wt% EG sample showed a 19-fold improvement in thermal conductivity. These results prove conclusively that alignment of the nanofillers in the polymer matrix significantly raises the thermal conductivity of the samples. However, unaligned samples also show a significant improvement and may be useful in applications when it is not possible to process in order to achieve nanoparticles alignment in the desired direction.

4. SUMMARY

Ultem™ was mixed with three different carbon-based nanofillers in efforts to increase the thermal conductivity of the polymer. After initial mixing, the nanocomposites were extruded or processed via the LMM process. HRSEM revealed significant alignment of the nanofillers in the extruded samples. Thermal conductivity measurements were made both in the direction and perpendicular to the direction of alignment of nanofillers as well as for unaligned samples. It was found that the largest improvement in thermal conductivity was achieved in the case of aligned samples when the measurement was performed in the direction of alignment. Unaligned samples also showed a significant improvement in thermal conductivity and may be useful in applications when it is not possible to align the nanofiller. However the improvements in thermal conductivity did not approach those expected based on a rule of mixtures. This is likely due to poor phonon transfer through the matrix.

5. ACKNOWLEDGEMENT

The authors would like to gratefully acknowledge Prof. Lawrence T. Drzal of Michigan State University for his valuable discussion. They would also like to thank Asbury Carbons for providing the EG and Tom Hughes of Applied Sciences, Inc. for providing the CNFs. Many thanks to Dr Craig M. Thompson, National Institute of Aerospace for reviewing the paper.

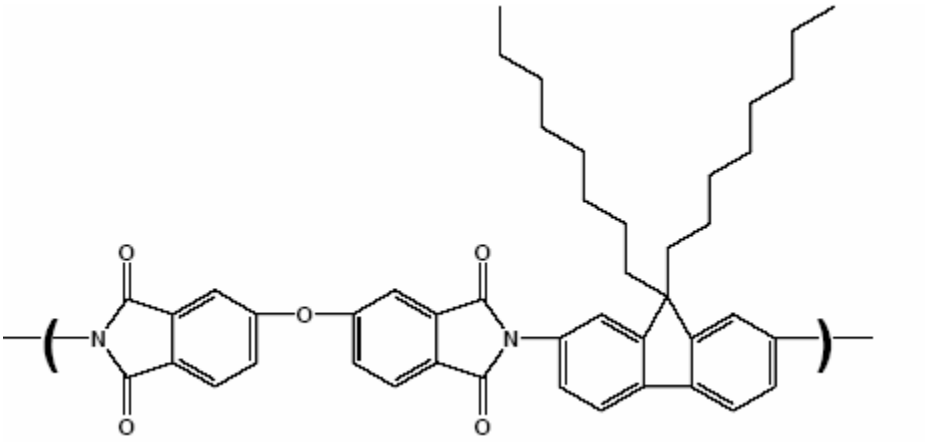

Figure 1. Chemical structure of polyimide dispersant

Figure 2. Ribbon of Ultem™/MWCNTs with arrow showing direction of tube alignment

Figure 3. Plaque showing cut direction and MWCNTs alignment (arrow)

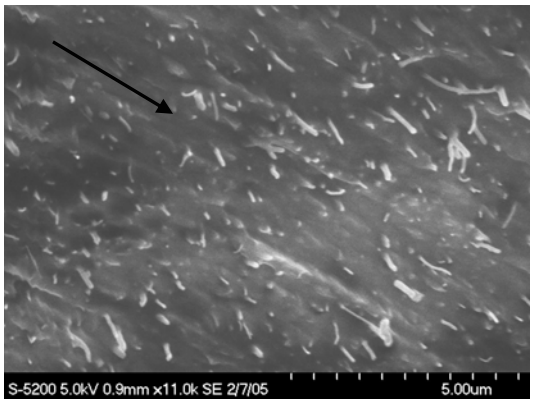

(a) Melt mixed

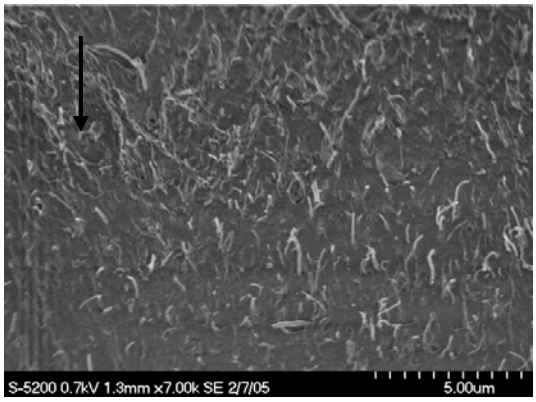

(b) Solution mixed

Figure 4: HRSEM of Ultem™/5 wt% MWCNTs ribbon sample; arrow denotes direction of flow

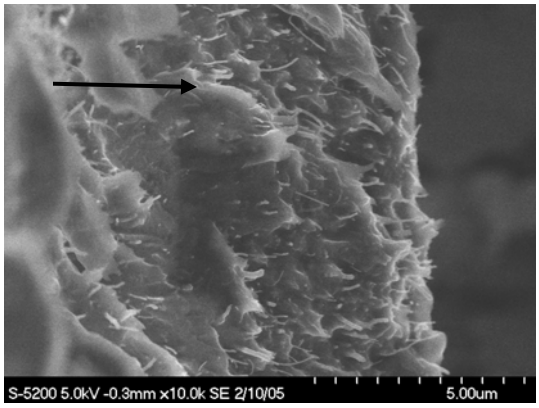

(a) 10 wt% MWCNTs melt mixed

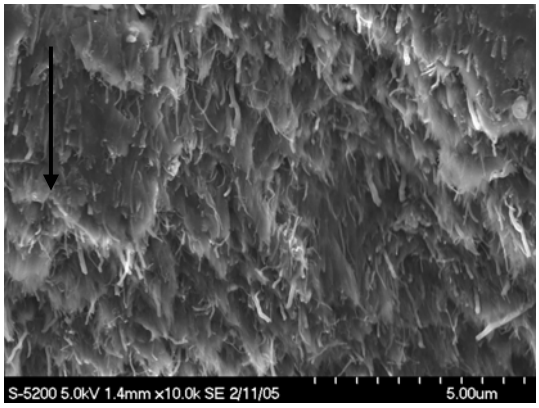

(b) 20 wt% MWCNTs melt mixed

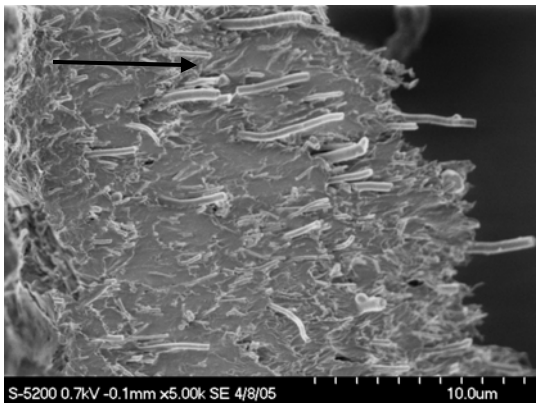

(c) 20 wt% CNFs melt mixed

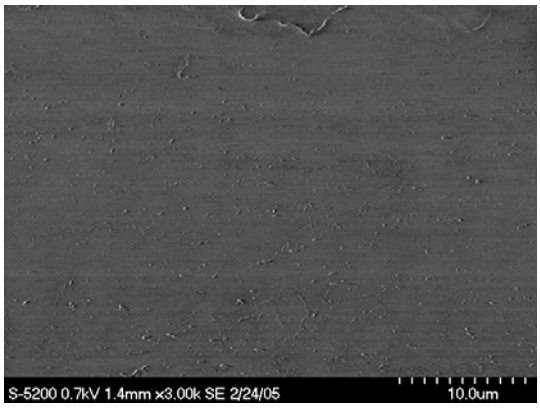

(d) 5 wt% MWCNTs melt mixed

Figure 5: HRSEM of Ultem™/nanofiller ribbon sample; arrow denotes direction of flow

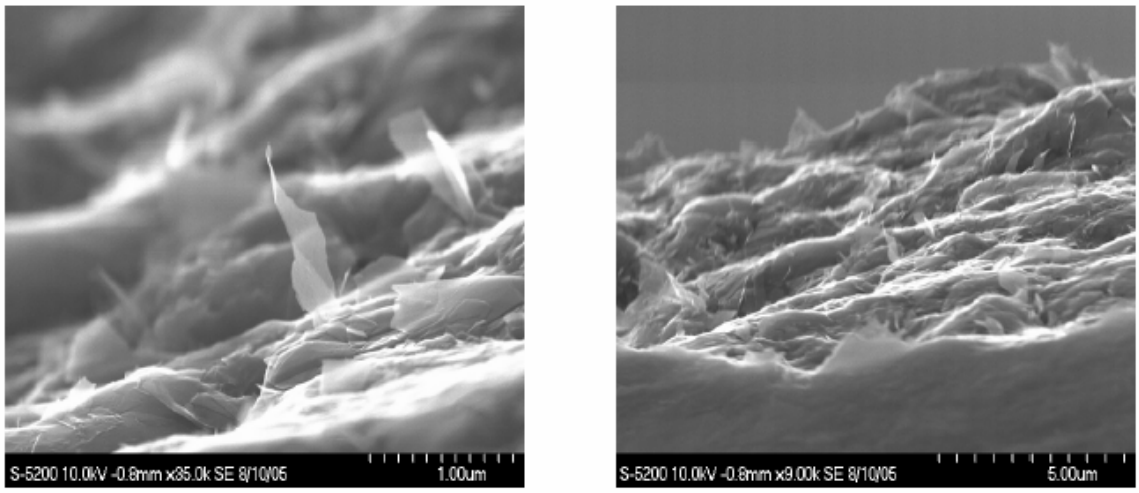

Figure 6: 40 wt% Asbury graphite in Ultem™ ribbon

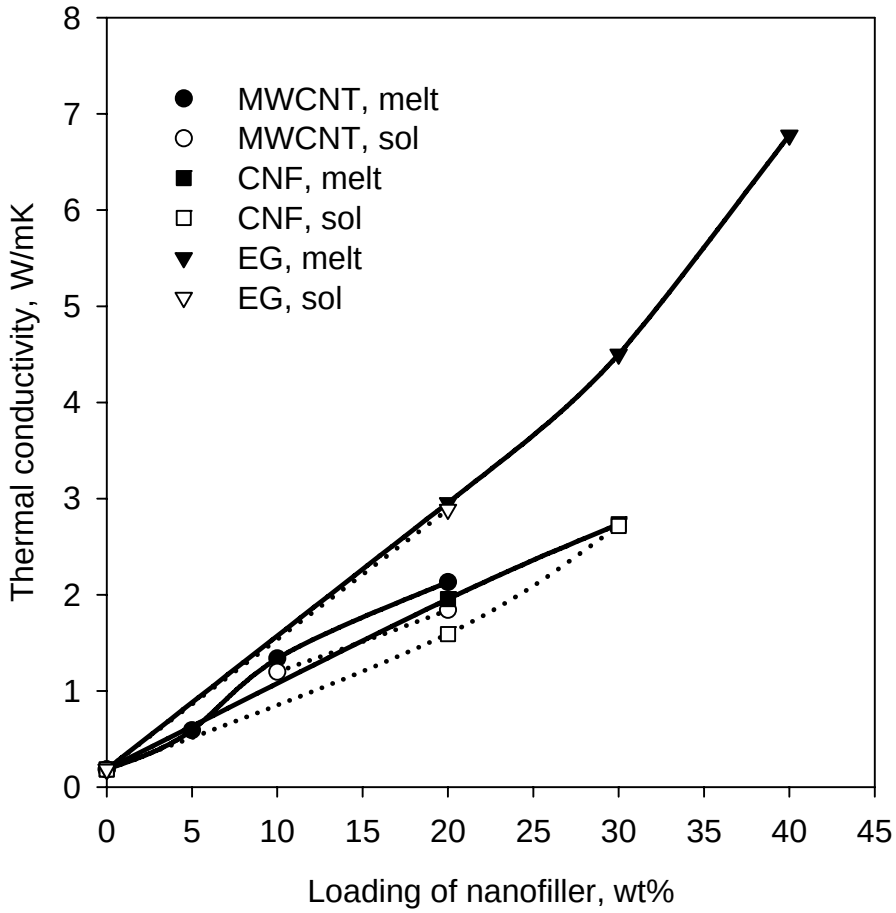

Figure 7: Thermal conductivity of molded Ultem™/nanofiller samples; measurement along direction of alignment

Table 1: Melt viscosities of Ultem™ 1000/nanofiller samples:

Sample	**Viscosity (poise)**
Neat Ultem™	37200
Ultem™, 5 wt% MWCNT	38000
Ultem™, 10 wt% MWCNT	47700
Ultem™, 20 wt% MWCNT	54700
Ultem™, 20 wt% CNF	35400
Ultem™, 30 wt% CNF	47200
Ultem™, 40 wt% CNF	50300
Ultem™, 20 wt% EG	31500
Ultem™, 30 wt% EG	37000
Ultem™, 40 wt% EG	46800
Ultem™, 50 wt% EG	57800

Shear rate: 92.5/sec, Temperature: 325 ^{o}C

Table 2: Mechanical properties of Ultem™/nanofiller samples:

Sample	**Modulus, GPa**	**Strength, MPa**	**Elong., %**
Ultem™ -- Neat	1.45 ± 0.05	49.64 ± 1.38	16 ± 11
Ultem™, 5 wt% MWCNT, melt	2.56 ± 0.12	91.70 ± 6.20	7 ± 0.5
Ultem™, 5 wt% MWCNT, sol.	--	--	--
Ultem™, 10 wt% MWCNT, melt	2.95 ± 0.17	72.39 ± 5.51	4 ± 1
Ultem™, 10 wt% MWCNT, sol.	1.19 ± 0.04	31.72 ± 2.07	3.5 ± 0.4
Ultem™, 20 wt% MWCNT, melt	3.50 ± 0.30	60.67 ± 11.72	2 ± .4
Ultem™, 20 wt% MWCNT, sol.	2.05 ± 0.23	58.61 ± 6.20	4 ± 0.5
Ultem™, 20 wt% CNF, melt	2.83 ± 0.30	48.26 ± 6.89	2 ± 0.3
Ultem™, 20 wt% CNF, sol.	2.24 ± 0.04	NA*	NA*
Ultem™, 30 wt% CNF, melt	3.76 ± 0.16	78.60 ± 5.52	3 ± 0.6
Ultem™, 30 wt% CNF, sol.	3.50 ± 0.10	64.12 ± 12.40	2.4 ± 0.7
Ultem™, 20 wt% EG, melt	5.40 ± 0.2	80.00 ± 13.00	2 ± 0.4
Ultem™, 20 wt% EG, sol.	4.70 (1 sample)	80	2.0
Ultem™, 30 wt% EG, melt	7.6 ± 0.3	96.5 ± 19.00	2 ± 0.5
Ultem™, 40 wt% EG, melt	--	--	--

*Ribbons were too thick for the 222.4 N (50 lb) load cell. Only modulus was obtained.

Table 3: Glass transition temperature (T_g) of Ultem™/nanofiller samples:

Sample	**Melt mixed, T_g (°C)**	**Solution mixed, T_g (°C)**
Ultem™, neat	216 (no mixing for neat)	
Ultem™, 5 wt% MWCNT	217	214
Ultem™, 10 wt% MWCNT	218	198
Ultem™, 20 wt% MWCNT	218	203
Ultem™, 20 wt% CNF	219	218
Ultem™, 30 wt% CNF	218	217
Ultem™, 20 wt% EG	218	217
Ultem™, 30 wt% EG	219	--
Ultem™, 40 wt% EG	219	--

Table 4a: Thermal conductivity of Ultem™/nanofiller extruded ribbons*:

Sample	**Thermal Conductivity, W/mK**
Neat Ultem™	0.172
Ultem™, 5 wt% MWCNT, melt	0.229
Ultem™, 5 wt% MWCNT, sol.	0.255
Ultem™, 10 wt% MWCNT, melt	0.272
Ultem™, 10 wt% MWCNT, sol.	0.192
Ultem™, 20 wt% MWCNT, melt	0.389
Ultem™, 20 wt% MWCNT, sol.	0.422
Ultem™, 20 wt% CNF, melt	0.364
Ultem™, 20 wt% CNF, sol.	0.386
Ultem™, 30 wt% CNF, melt	0.463
Ultem™, 30 wt% CNF, sol.	0.485
Ultem™, 20 wt% EG, melt	0.248
Ultem™, 20 wt% EG, sol.	0.356
Ultem™, 30 wt% EG, melt	0.287
Ultem™, 40 wt% EG, melt	0.387

* Thermal conductivity measurement is perpendicular to alignment

Table 4b: Thermal conductivity of Ultem™/nanofiller molded samples*:

Sample	**Thermal Conductivity, W/mK**
Neat Ultem™	0.184
Ultem™, 5 wt% MWCNT, melt	0.592
Ultem™, 5 wt% MWCNT, sol.	broken
Ultem™, 10 wt% MWCNT, melt	1.337
Ultem™, 10 wt% MWCNT, sol.	1.197
Sample	**Thermal Conductivity, W/mK**
Ultem™, 20 wt% MWCNT, melt	2.132
Ultem™, 20 wt% MWCNT, sol.	1.841
Ultem™, 20 wt% CNF, melt	1.955
Ultem™, 20 wt% CNF, sol.	1.592
Ultem™, 30 wt% CNF, melt	2.734
Ultem™, 30 wt% CNF, sol.	2.716
Ultem™, 20 wt% EG, melt	2.956
Ultem™, 20 wt% EG, sol.	2.886
Ultem™, 30 wt% EG, melt	4.499
Ultem™, 40 wt% EG, melt	6.777

* Thermal conductivity measurement is parallel to alignment

Table 4c: Thermal conductivity of Ultem™/nanofiller LMM samples (unoriented):

Sample	**Thermal Conductivity, W/mK**
Neat Ultem™	0.172
Ultem™, 20 wt% MWCNT, melt	0.500
Ultem™, 40 wt% CNF, melt	1.184
Ultem™, 40 wt% CNF, sol.	1.791
Ultem™, 20 wt% EG, melt	0.585
Ultem™, 30 wt% EG, melt	0.973
Ultem™, 40 wt% EG, melt	2.144
Ultem™, 50 wt% EG, melt	3.174

6. REFERENCES

1. J. Collister, Polymer Nanocomposites: Synthesis, Characterization and Modeling, Ed. R. Krishnamoorti and R.A. Vaia, ACS Symposium Series 804, (2002).
2. E. Hammel, X. Tang, M. Trampert, T. Schmitt, K. Mauthner, A. Eder and P. Potschke, Carbon, 42, 1153-1158 (2004).
3. K. Lozano, S. Yang and Q. Zeng, J. Appl. Poly. Sc., 93, 155-162 (2004).
4. R.J. Kuriger, M.K. Alam, D.P. Anderson and R.L. Jacobsen, Composites, Part A, 33, 53-62 (2002).
5. K. Lozano, J. Bonilla-Rios and E.V. Barrera, J. Appl. Poly. Sc., 79, 125-133 (2001).
6. O.S. Carneiro, J.A. Covas, C.A. Bernardo, G. Caldeira, F.W.J. Van Hattum, J.M. Ting, R.L. Alig and M.L. Lake; Composites Sc. Tech., 58, 401-407 (1998).
7. R.T. Pogue, J. Ye, D.A. Klosterman, A.S. Glass and R.P. Chartoff, Composites: Part A, 29, 1273 (1998).
8. C.A. Cooper, D. Ravich, D. Lips, J. Mayer and H.D. Wagner, Composites Sc. Tech., 62, 1105 (2002).
9. V.I. Merkulov, D.H. Lowndes, Y.Y. Wei, G. Eres and E. Voelkl, Appl Phys Lett, 76(24), 3555 (2000).
10. M. Endo, Y.A. Kim, T. Hayashi, Y. Fukai, K. Oshida, M. Terrones, T. Yanagisawa, S. Higaki and M.S. Dresselhaus, Appl Phys Lett, 80(7), 1267 (2002).
11. L.T. Drzal and H. Fukushima, Unites States Patent Application Publication, Pub No. US20040127621 (2004).
12. J.W. Shen, W.Y. Huang, S.W. Zuo and J. Hou, J.Appl. Polym. Sc., 97, 51-59 (2005).
13. W.Zheng, X. Lu and S.C. Wong, J. Appl. Polym. Sc., 91, 2781-2788, (2004).
14. G. Zheng, J. Wu, W. Wang and C. Pan, Carbon, 42, 2839-2847 (2004).
15. W. Zheng, S.C. Wong and H.J. Sue, Polymer, 73, 6767-6773, (2002).
16. L.N. Song, M. Xiao, X.H. Li and Y.Z. Meng, Mater. Chem, Phys., 93, 122-128, (2005).
17. D. Cho, S. Lee, G. Yang, H. Fukushima and L.T. Drzal, Macromol. Mater. Eng, 290, 179-187, (2005).
18. X. Gao, L. Liu, Q. Guo, J. Shi and G. Zhai, Materials Letters, 59, 3062-3065 (2005).
19. K.T. Lau and D. Hui, Composites Part B: Engineering, 33, 263-277 (2002).
20. C. Park, Z. Ounaies, K.A. Watson, R.E. Crooks, J.G. Smith Jr., S.E. Lowther, J.W. Connell, E.J. Siochi, J.S. Harrison and T.L. St. Clair, Chem. Phys. Lett.; 364, 303 (2002).
21. J.G. Smith Jr., J.W. Connell and P.M. Hergenrother, Soc. Adv. Matl and Proc. Eng. Proc.; 46: 510 (2001).
22. R. Haggenmueller, H.H. Gommans, A.G. Rinzler, J.E. Fischer and K.I. Winey, Chem Phys Lett; 330, 219 (2000).
23. R. Andrews, D. Jacques, M. Minot and T. Rantell, Macromol. Mater. Eng., 287(6), 395 (2002).
24. C.H. Liu, H. Huang, Y. Wu and S.S. Fan, Appl. Phys. Lett, 84, 4248-4250 (2004).
25. P. Kim, L. Shi, A. Majumdar and P.L. McEuen, Phys. Rev. Lett. 87 (21), 215502 (2001).
26. Y. J. Hwang, Y.C. Ahn, H.S. Shin, C.G. Lee, G.T. Kim, H.S. Park and J.K. Lee, Current Appl. Phys. article in press (2005).

27. S.U.S. Choi, Z.G. Zhang, W. Yu, F.E. Lockwood and E.A. Grulke, Appl. Phys. Lett, 79, 2252-2254 (2001).
28. M.A. Osman and D Srivastava, Nanotechnology, 12, 21-24 (2001).
29. Q Gong, Z. Li, X Bai, D. Li, Y. Zhao and J. Liang, Mater. Sc. Eng.A 384, 209-214 (2004).
30. E.J. Siochi, D.C. Working, C. Park, P.T. Lillehei, J.H. Rouse, C.T. Topping, A.R. Bhattacharya and S. Kumar, Composites: Part B; 35: 439, 2004.
31. H. Huang, C. Liu, Y. Wu and S. Fan, Adv. Mater (Communications), 17, 1652-1656 (2005).
32. S.T. Huxtable, D.G. Cahill, S. Shenogin. L. Xue, R. Ozisik, P. Barone, M. Usrey, M.S. Strano, G. Siddons, M. Shim and P. Keblinski, Nat. Mater., 11, 731-734 (2003).
33. Y.M. Chen and J.M. Ting, Carbon, 40, 359-362 (2002).